

# Characterization of Methacrylated Type-I Collagen as a Dynamic, Photoactive Hydrogel

Ian D. Gaudet · David I. Shreiber

Received: 28 November 2011 / Accepted: 23 February 2012 / Published online: 10 March 2012  
© The Author(s) 2012. This article is published with open access at Springerlink.com

**Abstract** Type-I collagen is an attractive scaffold material for tissue engineering due to its ability to self-assemble into a fibrillar hydrogel, its innate support of tissue cells through bioactive adhesion sites, and its biodegradability. However, a lack of control of material properties has hampered its utility as a scaffold. We have modified collagen via the addition of methacrylate groups to create collagen methacrylamide (CMA) using a synthesis reaction that allows retention of fundamental characteristics of native collagen, including spontaneous fibrillar self-assembly and enzymatic biodegradability. This method allows for a rapid, five-fold increase in storage modulus upon irradiation with 365 nm light. Fibrillar diameter of CMA was not significantly different from native collagen. Collagenolytic degradability of uncrosslinked CMA was minimally reduced, while photocrosslinked CMA was significantly more resistant to degradation. Live/Dead staining demonstrated that a large majority (71%) of encapsulated mesenchymal stem cells remained viable 24 h after photocrosslinking, which further increased to 81% after 72 h. This material represents a novel platform for creating mechanically heterogeneous environments.

## 1 Introduction

Hydrogels are semi-solid structures comprising networks of water-insoluble polymers surrounded by water [1]. Hydrogels are attractive materials for use as tissue

engineering scaffolds, particularly those made from materials that can polymerize in an aqueous environment that have potential to be injected into a defect or wound, and then polymerized to provide a stable matrix for cellular growth, remodeling, and regeneration into functional tissues [2–4]. Natural hydrogels from proteins such as collagen are both non-cytotoxic and highly biofunctional, but have somewhat constrained material properties and inherent variability in composition due to their biological origin, making them more difficult to work with from an engineering viewpoint [5–7]. Here, we aimed to use type-I collagen—the most abundant protein in the body that maintains excellent cytocompatibility and can self assemble into a fibrillar network [8]—as a base component for a photocrosslinkable biomaterial that can be mechanically tuned via application of light.

In recent years, the mechanical microenvironment has been elucidated as a potent modulator of cellular behavior and thus has been of great interest in designing scaffolds for tissue engineering [9–11]. In particular, stem cell-based tissue regeneration has shown scaffold mechanics to be of crucial importance in guiding and maintaining differentiation pathways [12, 13]. Synthetic scaffolds are increasingly popular, partly due to the ease with which their mechanical properties—as well as other characteristics—can be modulated. Natural materials such as collagen, while having the benefits of bioactivity, biodegradability, and cellular adhesivity, have been criticized for the limited control of their mechanical properties [14]. Collagen's mechanical properties have been extrinsically modulated in a variety of ways: by chemical crosslinking with agents such as glutaraldehyde [15], acyl azide [16], and genipin [17], by glycation modulation using reducing sugars [18], and by enzymatic crosslinking using either transglutaminase or lysyl oxidase [19, 20]. Although these methods have

I. D. Gaudet · D. I. Shreiber (✉)  
Department of Biomedical Engineering, Rutgers,  
The State University of New Jersey, 599 Taylor Road,  
Piscataway, NJ 08854, USA  
e-mail: shreiber@rci.rutgers.edu

varying degrees of success in augmenting the mechanical properties, issues of cytotoxicity, cost, and crosslinking time have been problematic in implementing these methods into collagen based scaffolds. Furthermore, all these methods are limited to applications where the crosslinking agent physically contacts the collagen, severely limiting spatial control of mechanical properties.

Over the last decade, synthetic photosensitive biomaterials have been developed to provide a platform in which application of light can be used to introduce spatiotemporal control of crosslink formation [21]. While the advantages of such synthetic materials include a high degree of control over material and chemical properties, they typically require additional modification to remain cell-tolerated and confer the bioactivity and degradability necessary for use as tissue regeneration scaffolds. More recently, natural biomaterials have been similarly modified to achieve a biomaterial with the innate benefits of natural materials with the high degree of control provided by photomanipulation [22, 23]. Photocrosslinking of fibrillar type-I collagen hydrogels has been also been pursued with a variety of methods, each with significant limitations. UV irradiation in the presence of flavin mononucleotide [24] produced only minimal changes in mechanical properties, and only when crosslinking was done prior to self-assembly. Collagen has also been modified via addition of photosensitive cinnamate groups [25], although the wavelength needed to crosslink is cytotoxic which prevents crosslinking in the presence of cells. Other approaches first modified collagen with either acrylate [26] or methacrylate [27] groups prior to photoinitiator-activated crosslinking. However, reaction conditions in these methods produced either unwanted gelation during reaction or partial denaturation of the collagen, resulting in significant changes in the fibrillar structure and the concomitant loss of desirable attributes such as bioactivity and biodegradability. Here, we describe and characterize a novel method for addition of photosensitive methacrylate groups to collagen that minimally compromises its ability to self-assemble into a biocompatible and bioactive hydrogel. This material provides a stable environment into which localized modifications can be made to the material properties of the scaffold.

## 2 Materials and Methods

### 2.1 Collagen Methacrylation

Type-I bovine collagen was modified by reacting free amines—primarily the  $\epsilon$ -amine groups on lysine residues, but also the  $\alpha$ -amine groups on the *N*-termini—with methacrylate groups to create collagen methacrylamide (CMA). 1-ethyl-3-(3-dimethylaminopropyl) carbodiimide

(EDC) and *N*-hydroxysuccinimide (NHS) in MES buffer were used to activate the carboxyl group of methacrylic acid (MA) for 10 min at 37°C, which was added to the collagen (3.75 mg/mL) in 0.02 N acetic acid and reacted for 24 h at 4°C. Following the reaction, the CMA was dialyzed against 0.02 N acetic acid, lyophilized for 72 h, and finally resuspended in 0.02 N acetic acid. Derivatization was verified using  $^1\text{H}$  NMR. NMR spectra were obtained with a Bruker Avance 360 MHz NMR. Lyophilized CMA was dissolved in deuterated DMSO (10 mg/mL) overnight and NMR spectra were calibrated to the residual solvent peak (2.50 ppm). Derivatization efficiency was also evaluated using a trinitrobenzenesulfonic acid (TNBSA) assay, modified from Sheu et al. [28] to quantify the free amines present before and after derivatization. All chemicals were purchased from Sigma-Aldrich unless otherwise specified. Native type-I collagen that was not reacted with methacrylic acid was used as a control.

### 2.2 UV Rheometry

CMA was mixed in 1 mL batches, in which 677  $\mu\text{L}$  CMA (3.75 mg/mL) was added to 20  $\mu\text{L}$  HEPES, 140  $\mu\text{L}$  0.15 N NaOH, 100  $\mu\text{L}$  10 $\times$  PBS, 53  $\mu\text{L}$  PBS, and 10  $\mu\text{L}$  of a photoinitiator solution containing 2.5% (w/v) Irgacure 2959 (I2959) in methanol. This collagen solution was immediately loaded into a 600  $\mu\text{m}$  gap between a 20 mm top parallel plate and a quartz lower plate on a modified Kinexus Ultra rotational rheometer (Malvern Instruments, Worcestershire, UK) (Fig. 1). The temperature was raised to 37°C with a Peltier-controlled stage to induce fibrillogenesis. After 10 min the sample was exposed to UV light (365 nm, 100 mW/cm<sup>2</sup>) through the quartz bottom plate for various exposure periods to photocrosslink the gel.

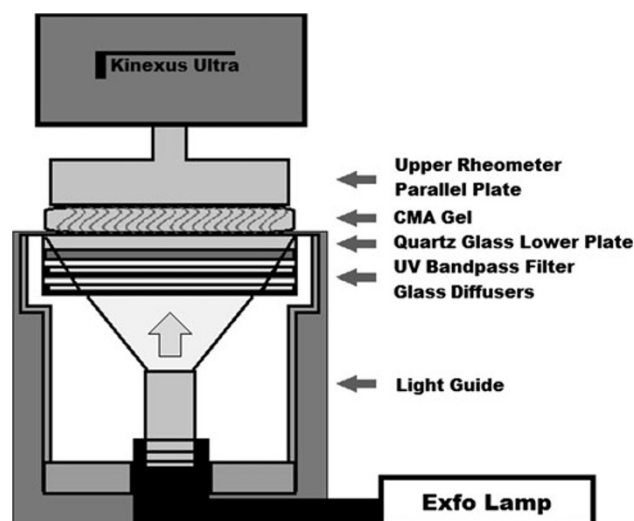


**Fig. 1** Schematic of UV Rheometry setup

Throughout this process, and continuing for 20 min, the sample was oscillated (0.5% strain, 1 rad/s), and the resultant torque was measured to obtain mechanical properties of the material during both self-assembly and photocrosslinking.

### 2.3 Scanning Electron Microscopy

Native collagen and CMA gels were prepared as above, except on glass coverslips. Following self-assembly and photocrosslinking, gels were dehydrated in a series of aqueous acetone solutions (25, 50, 75, 95, 100%) and critical point dried (CPD 020, Balzers Union Limited, Balzers, Liechtenstein). Samples were then sputter coated with gold/palladium (SCD 004, Balzers Union Limited, Balzers, Liechtenstein) and imaged via SEM (Amray 1830I, Amray Inc. Bedford, MA). Fibril diameter was measured on 20 separate images per condition. Diameter was sampled on fibrils at the grid intersections of an overlaid  $8 \times 12$  grid, and measured using ImageJ (ImageJ, NIH, Bethesda, MD).

### 2.4 Circular Dichroism (CD) Spectroscopy

CD spectroscopy was performed using an Aviv Model 400 Spectropolarimeter (Aviv Biomedical Inc., Lakewood, NJ). Native collagen and CMA at 0.1 mg/mL, along with a reference sample of 0.02 N acetic acid buffer, were injected into a quartz glass cuvette with a 1 mm path length. Ellipticity was averaged over 10 s and recorded from 290 nm down to 190 nm in 1 nm intervals. All samples were run at 10°C.

### 2.5 Collagenase Degradation: Rheology and BCA

Degradation of the mechanical properties of gels was evaluated via reduction in storage modulus ( $G'$ ) due to enzymatic cleavage of collagen fibrils. For rheological analysis during enzymatic degradation, collagen or CMA solutions were prepared as above and loaded onto the rheometer in a poly(dimethyl siloxane) (PDMS) ring, allowed to gel at 37°C, and exposed to UV for crosslinking. Samples were then cooled to 15°C and Type-I collagenase (0.1 mg/mL) was added and allowed to diffuse into the gel for 5 min. After aspiration of excess collagenase, the upper parallel plate was lowered onto the gels, temperature was returned to 37°C, and the sample was exposed to 3 s of oscillatory shear (1 rad/s, 0.5% strain) every 5 min for 1 h. Degradation of the fibrillar structure was evaluated with a separate assay, adapted from Daminik et al. [29]. Collagenase (0.01 mg/mL) was added to gelled and photocrosslinked collagen and CMA in a 96-well plate, where

samples of the gel supernatant were removed every 30 min and the total liberated protein determined by BCA assay.

### 2.6 Cytotoxicity Testing

Adult human mesenchymal stem cells (hMSC) were expanded in tissue culture flasks for 7 days in  $\alpha$ -MEM (Invitrogen, Carlsbad, CA) supplemented with 20% FBS (Atlanta Biologicals, Norcross, GA), 1% penicillin/streptomycin, and 2 ng/mL bFGF (Peprotech, Rocky Hill, NJ). Following expansion, hMSC were detached via trypsin/EDTA, washed in culture media, and encapsulated at a density of  $1 \times 10^5$  cells/mL within native collagen without photoinitiator or CMA gels containing 0.025% I2959. Gels were exposed to UV for 90 s, and returned to culture for 24 or 72 h. After the culture period, cells were labeled with Hoechst 33342, Calcein-AM, and ethidium homodimer. Fluorescent microscopy was used to visually assess cellular viability based on intercellular cleavage of calcein-AM to calcein (live) or uptake of ethidium into the nucleus (dead). Hoechst 33342 was used to visualize all nuclei. Image intensities were set at a predetermined threshold, from which live and dead cells were quantified using the Particle Analyzer function in ImageJ.

### 2.7 Statistical Analyses

Data were analyzed for statistical significance using a one-way ANOVA, significance level  $P < 0.05$ , and the Tukey post hoc test for pairwise comparisons (Kaleidagraph v4.1, Synergy Software, Reading, PA).

## 3 Results

### 3.1 Functionalization

Proton NMR detected large peaks at 5.3 and 5.6 ppm, indicating that methacrylate derivatization to free amines was successful. Additional smaller peaks near 6 ppm suggested that derivatization of other less prevalent reactive side groups occurred as well (Fig. 2a). NMR spectra are otherwise nearly identical to native collagen, verifying that no other significant reactions occurred during the synthesis and purification process (Fig. 2b). Quantification of free amines using TNBSA showed that approximately 20% of the free amines were converted to methacrylamide groups (data not shown).

### 3.2 Rheology

Rheological analysis (Fig. 3) of CMA gels demonstrates self-assembly of the material into a fibrillar hydrogel as

**Fig. 2**  $^1\text{H}$  NMR spectra of CMA and Native Type-I collagen. Hydrogen atoms on methacrylate moieties of CMA (a), are present as peaks (5.3–6.3 ppm). These peaks are absent on the spectrum of native type-I collagen (b); otherwise spectra are similar

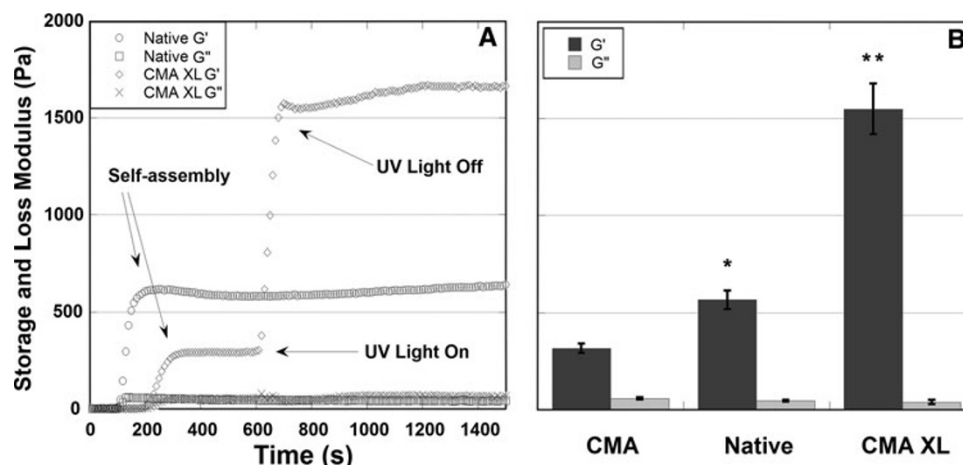
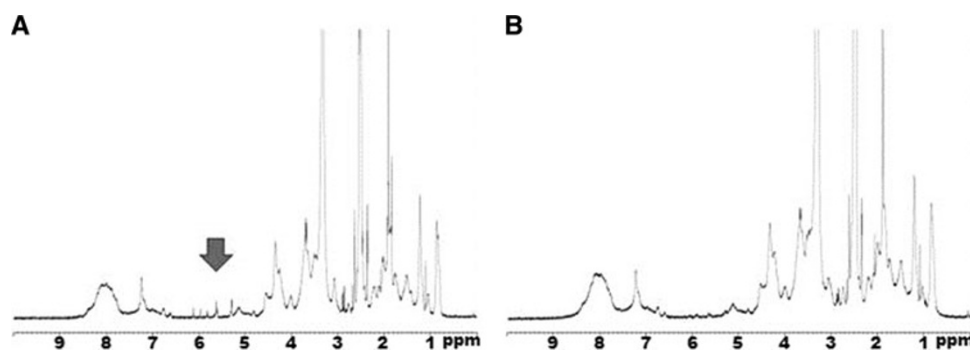


**Fig. 3** Real-time rheological data (a) of native collagen (open circle  $G'$ , open square  $G''$ ) and CMA (open diamond  $G'$ , "x"  $G''$ ) during self-assembly and photocrosslinking. Self assembly is seen as a rise in  $G'$  from  $t = 150$ – $300$  s. Photocrosslinking is seen as a large increase in  $G'$  following 60 s UV exposure starting at  $t = 600$  s.  $G'$  and  $G''$  curves shown are representative samples. Average equilibration

values of  $G'$  and  $G''$  (b). CMA and native values were taken at  $t = 10$  min, crosslinked (XL) CMA values are taken 10 min after UV exposure. Error bars are  $\pm$ SD. Single asterisk is significantly different than CMA; double asterisk is significantly different than native and CMA,  $P < 0.05$ , ANOVA followed by Tukey's post hoc test

evidenced by the increase in storage modulus around 200–300 s after incubation at 37°C. The kinetics of self-assembly were slightly delayed compared to native collagen, which self-assembled from 100 to 200 s following the temperature increase. Photolabile functionality of CMA was demonstrated by the rapid, five-fold increase in storage modulus ( $G'$ ) upon irradiation with UV light in the presence of photoinitiator. A small, oscillatory increase in the loss modulus ( $G''$ ) was observed during irradiation, however after the 90 s exposure period, the equilibrium loss modulus was slightly lower than prior to photocrosslinking. The large increase in storage modulus from pre-crosslinked ( $323.4 \pm 7.8$  Pa at  $t = 600$  s) to post-crosslinked ( $1,316.8 \pm 51.3$  Pa at  $t = 1,200$  s) along with the slight decrease in loss modulus ( $57.7 \pm 4$  Pa to  $39.8 \pm 6.5$  Pa) indicates that photocrosslinking of CMA results in a mechanically stiffer and more elastic material. Tunability of CMA via UV exposure time is demonstrated in Fig. 4a. Exposure for 30, 45, and 90 s resulted in a 30, 60, and 100% increase in

storage modulus. Figure 4b displays dynamic control of the material, as six distinct 15 s UV exposure periods incrementally increased the storage modulus ( $\sim 5, 30, 60, 80, 90, 100\%$  of maximum) while maintaining a stable modulus immediately after removal of light.

### 3.3 Scanning Electron Microscopy

SEM revealed similar fiber formation for CMA and native type-I collagen as well as photo-crosslinked CMA (Fig. 5a–c). No substantial differences in fiber size, orientation, or quantity were observed, further indicating that the methacrylation reaction largely preserves the quaternary structure of the collagen, and that the photocrosslinking process does not significantly alter the fibrillar ultrastructure. Quantification of fiber diameter (Fig. 5d) confirmed that there were no statistical differences in average diameter or size distribution.



**Fig. 4** Real-time rheological data. (a) CMA exposed to UV light for 30, 45, and 90 s shows that light exposure time can be used to precisely tune the storage modulus to a set value. (b) Applying sequential, discrete exposure periods changes the storage modulus dynamically. Arrows indicate 15 s UV exposures, followed by 75 s without UV

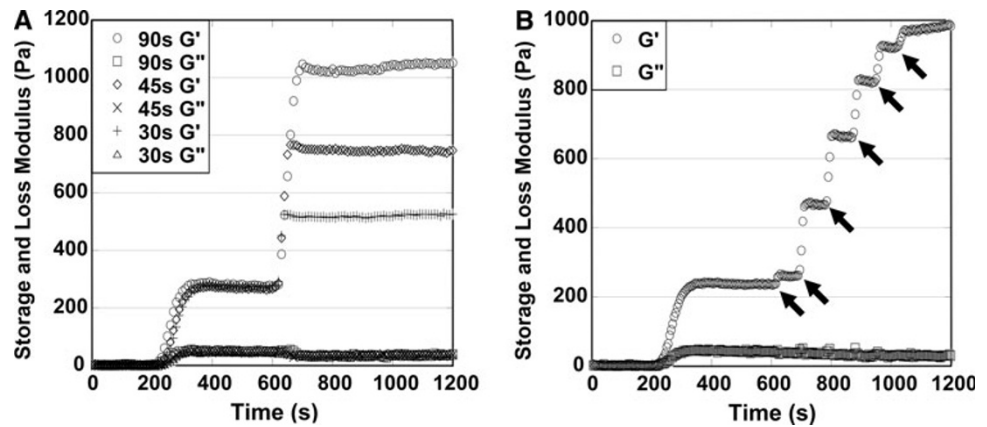
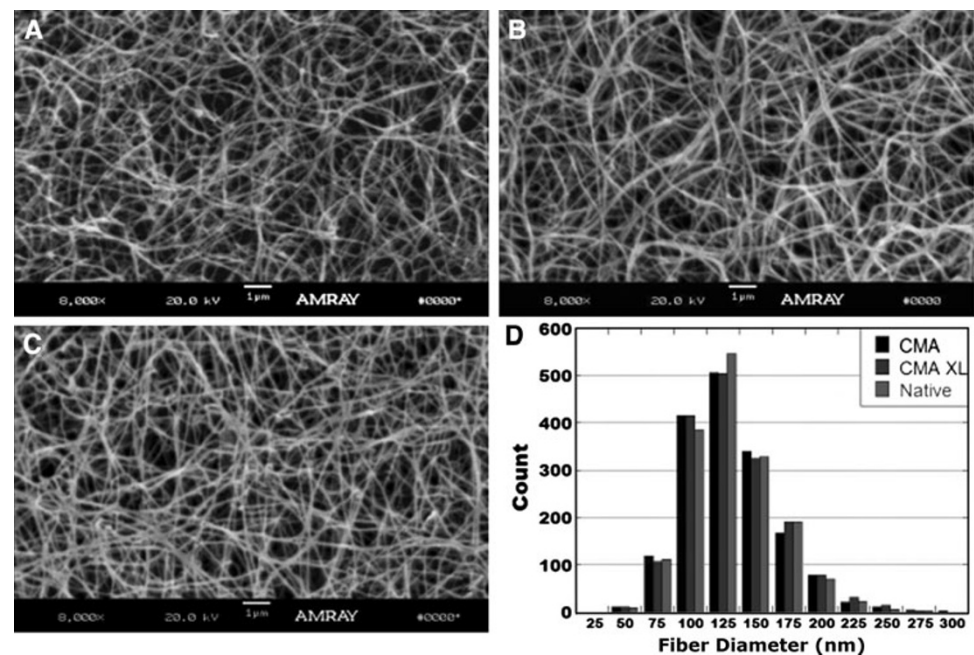


**Fig. 5** SEM images of (a) CMA, (b) Photocrosslinked CMA, and (c) native collagen. Images are  $\times 8,000$ , scale bar 1  $\mu\text{m}$ . Histogram (d) shows diameter distribution in 25 nm bins



### 3.4 CD Spectroscopy

The ellipticity of CMA as compared to native collagen presented no significant differences at the characteristic 221 nm peak, indicating an equal concentration of  $\alpha$ -helix in both materials (Fig. 6).

### 3.5 Collagen Degradation

Collagenase degradation assays were performed to assess whether the derivatization reaction or the photocrosslinking process had an effect on enzymatic degradation of the gels (Fig. 7). The rate of mechanical degradation rate, reported here as the reduction in storage modulus as a percentage of initial storage modulus over time, was not statistically different between native collagen and CMA, indicating similar degradation kinetics. However, the

degradation rate of photocrosslinked CMA was significantly lower ( $P < 0.05$ ) than both native collagen and uncrosslinked CMA. A separate collagenase test assayed the percent of protein liberated from the gels following 3 h of exposure to collagenase. Native collagen ( $72.8 \pm 0.2\%$  protein liberated) was most degraded after 3 h, followed by CMA ( $55 \pm 2.8\%$ ), and finally photocrosslinked CMA ( $35.9 \pm 4\%$ ).

### 3.6 Cytotoxicity

The tolerance of entrapped hMSCs to the photocrosslinking process was evaluated 24 (Fig. 8) and 72 h after exposure to UV light. As outlined in Fig. 9, minimal cell death was observed in the control condition of native collagen ( $98 \pm 1$  and  $97 \pm 1\%$  viable at 24 and 72 h, respectively) without UV/photoinitiator exposure, whereas in the

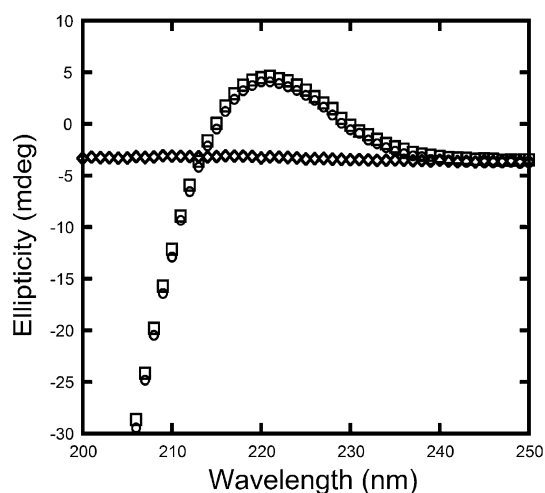


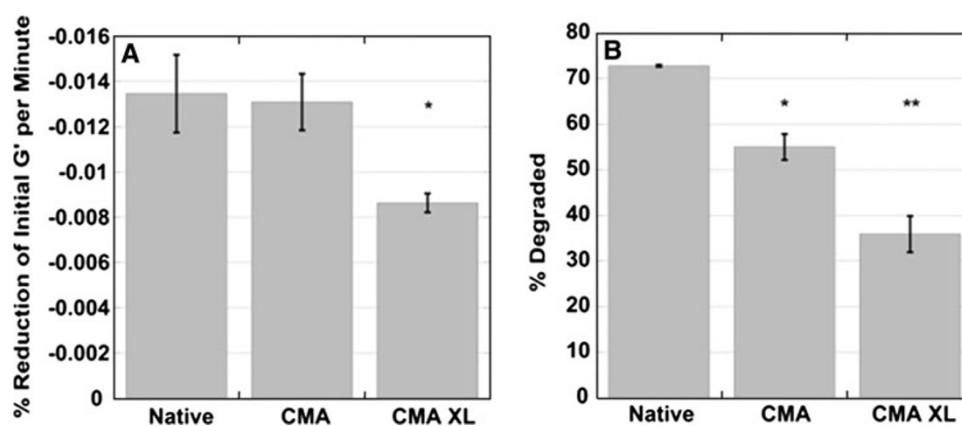
**Fig. 6** CD spectra of native collagen (*open circle*) and CMA (*open square*) displaying the characteristic peak at 221 nm indicative of the presence of  $\alpha$ -helical structure. 0.02 N acetic acid (*open diamond*) was included as the reference buffer

photocrosslinked CMA condition there was a significant drop in viability ( $71 \pm 5\%$ ) at 24 h that recovered to  $81 \pm 2\%$  at 72 h. There was no significant difference in total cell number between any of the groups. Activation of the photoinitiator in the presence of hMSC within CMA has a noticeable effect on cellular viability, although a large majority of the photocrosslinked cells were viable at both time points.

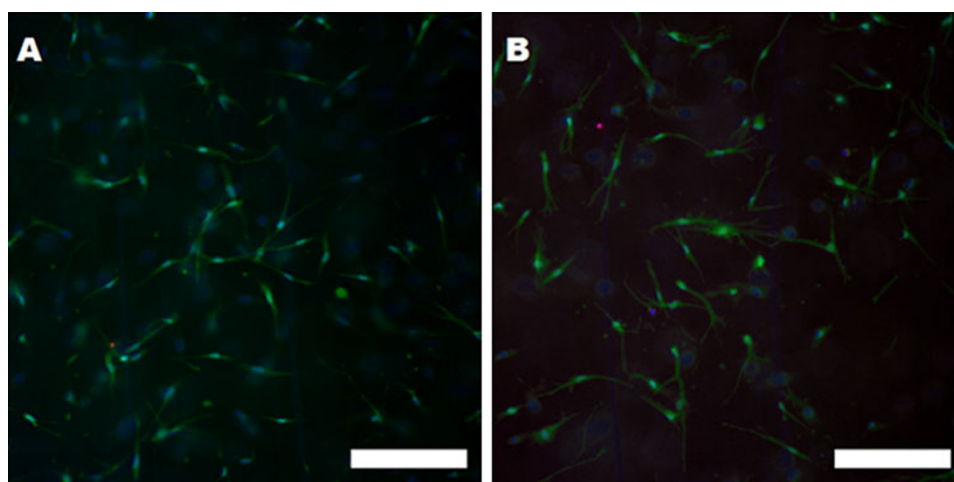
#### 4 Discussion

We have developed and characterized a robust, photosensitive material based on type-I collagen to modulate mechanical properties via the application of light. The method to synthesize CMA derivatizes a large percentage of free amines with reactive methacrylate groups without significantly altering the structural and functional properties that make type-I collagen an attractive and versatile scaffold

**Fig. 7** Collagenase degradation assay data. **(a)** Rheological collagenase assay. *Bars* represent slope from a linear fit of percent of initial storage modulus versus time over the 2 h test. **(b)** BCA assay for determination of collagen liberation due to collagenolytic degradation. *Bars* represent percent of original mass of gels in solution after 3 h test. *Error bars* are  $\pm$ SD,  $N = 3$ .  $P < 0.05$



**Fig. 8** Cytocompatibility of hMSC encapsulated in **(a)** native collagen or **(b)** photocrosslinked CMA. Images taken 24 h after UV exposure. *Green* (Live) is Calcein AM, *Red* (Dead) is Ethidium Homodimer, *Blue* (Nuclei) is Hoechst 33342. *Scale bar* 200  $\mu$ m



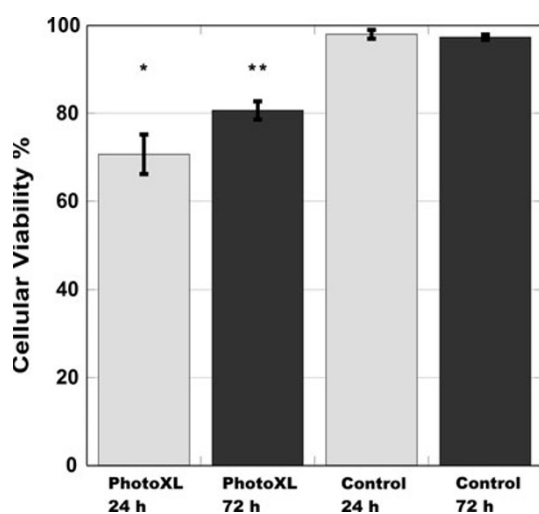


**Fig. 9** Quantification of hMSC viability at 24 and 72 h after encapsulation and/or photocrosslinking. Photo XL is photocrosslinked, while Control is native collagen without exposure to UV or I2959

material. CMA is able to self-assemble from a liquid macromer solution into a fibrillar hydrogel at physiological pH and temperature, with similar assembly kinetics and resultant structure as compared to native type-I collagen, although the onset of self-assembly of CMA following the temperature ramp is delayed. This discrepancy might be caused by subtle changes in the protein structure, by derivitization of *N*-termini free amines, or by loss of low-molecular weight protein fragments during dialysis. Both CMA and native collagen formed mechanically stable gels less than 10 min after temperature increase. Following photocrosslinking for 90 s, the storage modulus of the crosslinked CMA is almost three times that of native collagen at the same concentration. However, the storage modulus of uncrosslinked CMA hydrogels is slightly lower than that of native collagen, potentially due to unwanted crosslinking of collagen molecules during the synthesis reaction. Another possibility is that the reduction in storage modulus is due to the loss of intrafibril ionic associations between the positively charged amine groups and negatively charged residues [30]. Analysis of tertiary and quaternary structure through CD spectroscopy and SEM suggests the former, as  $\alpha$ -helix content and fibril diameter distribution were essentially identical between native collagen and CMA. Additionally, there were occasional rosette-like structures within the CMA gels that appeared to be due to branching incidents during self-assembly, which could be a result of multiple collagen molecules being crosslinked during the CMA synthesis reaction. These rosettes may potentially disrupt the local mechanical properties of the gels by forming small discontinuities within the fibrous network that may be prone to microscopic tears, thus resulting in a lower bulk storage modulus. This reduction in bulk material properties can be

offset by altering the initial CMA concentration. However, there is the possibility that localized differences in material properties exist at the microscale, and these pockets of heterogeneity may have undesired consequences with respect to the cell matrix interface. A more in depth examination of the mechanical microenvironment with a more appropriate testing modality such as atomic force microscopy [31] may help elucidate these questions in the future.

Collagenase degradation assays were performed to determine if the methacrylate derivatization had any effect on the enzymatic degradation of the CMA gels before crosslinking, and if photocrosslinked CMA gels were significantly less degradable than the uncrosslinked CMA and native collagen samples. Since type-I collagenase requires an intact triple helix to effectively degrade fibrillar collagen, if the tertiary structure was indeed altered significantly then collagenase degradation rates should also be affected, which may influence the biodegradability of the material as well as the extent that cells may remodel the scaffold [32]. Also, crosslinking of collagen has previously been shown to decrease the collagenolytic degradation rate, as crosslinks between collagen molecules increase the number of ligations necessary to liberate protein fragments and affects the availability of recognizable triple helical segments [33, 34]. We evaluated separately the mechanical degradation and the chemical degradation of pre- and post-photocrosslinked CMA gels as compared to native collagen. Rheological testing was performed to evaluate the percent reduction in initial storage modulus over time during a continuous hour-long test. Chemical degradation was assessed via sampling collagenase-exposed gels over a 3 h period. Rheological tests showed that the mechanical degradation rate was not statistically significant between native and uncrosslinked CMA gels, while photocrosslinked CMA gels showed a significantly lower degradation rate ( $P < 0.05$ ). The chemical degradation assay indicated that the degradation rate of CMA was lower than that of native collagen gel, and that crosslinking CMA further decreased the degradation rate. This apparent discrepancy between the rheological and chemical assays may again be attributed to ectopic crosslinks that result in anomalous structure formation during fibrillogenesis. These structures may be protected from collagenase degradation by a lack of enzyme binding sites as well as stabilizing covalent bonds. Thus, they are not liberated into solution, as seen by the BCA assay, and do not contribute to the mechanical strength of the gels. As such their lack of degradation has no effect on the storage modulus during the rheological collagenase degradation assay. Most importantly, in both assays the photocrosslinked CMA was significantly less degradable. This aspect may prove extremely useful, as photocrosslinking may be exploited to spatially control the degradation rate of individual regions of the scaffold.

Preliminary cytocompatibility screening demonstrated that methacrylate derivatization had no apparent impact on cellular compatibility. Previous studies have shown that the photoinitiator used here, I2959, is generally tolerated by hMSC at the concentrations used, although some cell types are more susceptible than others [35, 36]. In our system, the photocrosslinking process also appears to be well tolerated by hMSC, although an increase in ethidium-positive cells was observed in CMA gels 24 and 72 h after photocrosslinking as compared to cells in native collagen gels without photoinitiator activation. While the free radicals produced during photocrosslinking induced some cell death, the majority of cells in the gel were viable at both time points, with viability improving from 24 to 72 h. This observation is encouraging, as it implies that modulation of CMA scaffolds can be conducted in the presence of encapsulated cells, allowing for in situ modification of these injectable cellularized scaffolds. However, it still remains to be seen how exposure to the radicals generated during crosslinking influences the differentiation fate, and these effects will need to be decoupled from those imparted to the micro-niche as a result of the mechanical modulation.

## 5 Conclusions

We have created and characterized a novel method for derivatizing type-I collagen with photocrosslinkable methacrylate groups, resulting in a robust material that can be mechanically tuned via the application of light in the presence of live cells. We observed a fivefold increase in the storage modulus with application of UV light for only 90 s, and the change in stiffness can be easily tuned by adjusting the amount of UV exposure. Our laboratory has previously shown that modulation of the mechanical properties of collagen via chemical crosslinking provides cues that can be used to direct cellular behavior [37]. While a multitude of strategies exist for chemically crosslinking collagen to affect bulk material properties [38, 39], these techniques cannot easily be applied in a localized manner, nor can they affect the properties as rapidly. The power to locally tune the mechanical properties within a gel is desirable for creating a soft-tissue scaffold with controlled heterogeneity. This material largely retains the characteristic structure and attributes of fibrillar collagen while also being mechanically dynamic, resulting in a self-assembling, bioactive, biocompatible hydrogel that provides a high degree of spatial material control. We believe this material has utility as a potential scaffold for regenerating soft tissues with irregularly shaped defects which require an injectable, self-assembling scaffold to fill the wound site without further disruption of nearby viable tissue. This material may be particularly useful as a scaffold material

for hMSC-based therapies for nervous system injuries, as the range of stiffness allowed from uncrosslinked to crosslinked CMA is similar to that of native CNS tissue [40]. The mechanical microenvironment has been shown to strongly direct hMSC differentiation [41], and the power to spatially control the mechanical properties of the scaffold may provide a useful tool for differentiation of progenitor cells into multi-cellular tissues with specified architectures. This system is especially amenable for use with hMSC, as they may be able to withstand the free-radical induced damage more readily than other progenitor cell types due to their relatively low proliferation rate and innate propensity to mitigate radical and oxidative damage [42]. Following stabilization of the hydrogel within the defect, mechanical heterogeneity may be introduced, allowing the creation of complex, customizable scaffolds that mimic the structure of the lost tissue and increase the chance of restoring function by recapitulating some aspects of the original tissue.

**Acknowledgments** Special thanks to Dr. Joshua Katz and Dr. Jason Burdick and for their assistance in obtaining proton NMR spectra and Dr. Jens Volker for his help obtaining CD spectra. The authors would like to thank the New Jersey Commission on Spinal Cord Research Fellowship #08-2937-SCR-E-0, National Science Foundation Grant #ARRA-CBET0846328, and NSF IGERT DGE Grant #0801620 for their generous support. Some of the materials employed in this work were provided by the Texas A&M Health Science Center College of Medicine Institute for Regenerative Medicine at Scott & White through a grant from NCRR of the NIH, Grant #P40RR017447.

**Open Access** This article is distributed under the terms of the Creative Commons Attribution License which permits any use, distribution, and reproduction in any medium, provided the original author(s) and the source are credited.

## References

1. Lee KY, Mooney DJ (2001) Hydrogels for tissue engineering. *Chem Rev* 101(7):1869–1880. doi:10.1021/cr000108x
2. Nicodemus GD, Bryant SJ (2008) Cell encapsulation in biodegradable hydrogels for tissue engineering applications. *Tissue Eng Pt B-Rev* 14(2):149–165
3. Bryant SJ, Bender RJ, Durand KL, Anseth KS (2004) Encapsulating Chondrocytes in degrading PEG hydrogels with high modulus: engineering gel structural changes to facilitate cartilaginous tissue production. *Biotechnol Bioeng* 86(7):747–755. doi:10.1002/bit.20160
4. Jen AC, Wake MC, Mikos AG (1996) Review: hydrogels for cell immobilization. *Biotechnol Bioeng* 50(4):357–364
5. Cheung DT, Perelman N, Ko EC, Nimmi ME (1985) Mechanism of crosslinking of proteins by glutaraldehyde.3. reaction with collagen in tissues. *Connect Tissue Res* 13(2):109–115
6. Cen L, Liu W, Cui L, Zhang WJ, Cao YL (2008) Collagen tissue engineering: development of novel biomaterials and applications. *Pediatr Res* 63(5):492–496
7. Yang L, Van der Werf KO, Fitie CFC, Bennink ML, Dijkstra PJ, Feijen J (2008) Mechanical properties of native and cross-linked type-I collagen fibrils. *Biophys J* 94(6):2204–2211. doi:10.1529/biophysj.107.111013



8. Rest Mvd, Garrone R, Herbage D (1993) Collagen: a family of proteins with many facets. In: Bittar EE (ed) *Advances in molecular and cell biology*, vol 6. Elsevier, Amsterdam, pp 1–67
9. Levenberg S, Dado D (2009) Cell-scaffold mechanical interplay within engineered tissue. *Semin Cell Dev Biol* 20(6):656–664. doi:[10.1016/j.semcdb.2009.02.001](https://doi.org/10.1016/j.semcdb.2009.02.001)
10. Discher DE, Janmey P, Wang Y-I (2005) Tissue cells feel and respond to the stiffness of their substrate. *Science* 310(5751):1139–1143. doi:[10.1126/science.1116995](https://doi.org/10.1126/science.1116995)
11. Rehfeldt F, Engler AJ, Eckhardt A, Ahmed F, Discher DE (2007) Cell responses to the mechanochemical microenvironment—Implications for regenerative medicine and drug delivery. *Adv Drug Deliv Rev* 59(13):1329–1339. doi:[10.1016/j.addr.2007.08.007](https://doi.org/10.1016/j.addr.2007.08.007)
12. O'Connor KC, Barrilleaux B, Phinney DG, Prockop DJ (2006) Review: ex vivo engineering of living tissues with adult stem cells. *Tissue Eng* 12(11):3007–3019
13. Discher DE, Engler A, Carag C, Rehfeldt F (2008) Matrix elasticity effects on cardiomyocytes and stem cells: Similarities, differences and therapeutic implications. *Biorheology* 45(1–2):54
14. Lau KT, Cheung HY, Lu TP, Hui D (2007) A critical review on polymer-based bio-engineered materials for scaffold development. *Compos Part B-Eng* 38(3):291–300. doi:[10.1016/j.compositesb.2006.06.014](https://doi.org/10.1016/j.compositesb.2006.06.014)
15. Olde Damink LHH, Dijkstra PJ, Luyn MJA, Wachem PB, Nieuwenhuis P, Feijen J (1995) Glutaraldehyde as a crosslinking agent for collagen-based biomaterials. *J Mater Sci Mater Med* 6(8):460–472. doi:[10.1007/bf00123371](https://doi.org/10.1007/bf00123371)
16. Simmons DM, Kearney JN (1993) Evaluation of collagen cross-linking techniques for the stabilization of tissue matrices. *Biotechnol Appl Biochem* 17(1):23–29. doi:[10.1111/j.1470-8744.1993.tb00229.x](https://doi.org/10.1111/j.1470-8744.1993.tb00229.x)
17. Bigi A, Cojazzi G, Panzavolta S, Roveri N, Rubini K (2002) Stabilization of gelatin films by crosslinking with genipin. *Biomaterials* 23(24):4827–4832
18. Tranquillo RT, Girton TS, Oegema TR (1999) Exploiting glycation to stiffen and strengthen tissue equivalents for tissue engineering. *J Biomed Mater Res* 46(1):87–92
19. Orban JM, Wilson LB, Kofroth JA, El-Kurdi MS, Maul TM, Vorp DA (2004) Crosslinking of collagen gels by transglutaminase. *J Biomed Mater Res Part A* 68A(4):756–762. doi:[10.1002/jbm.a.20110](https://doi.org/10.1002/jbm.a.20110)
20. Siegel RC, Pinnell SR, Martin GR (1970) Cross-linking of collagen and elastin: Properties of lysyl oxidase. *Biochemistry* 9(23):4486–4492. doi:[10.1021/bi00825a004](https://doi.org/10.1021/bi00825a004)
21. Ifkovits JL, Burdick JA (2007) Review: photopolymerizable and degradable biomaterials for tissue engineering applications. *Tissue Eng* 13(10):2369–2385. doi:[10.1089/ten.2007.0093](https://doi.org/10.1089/ten.2007.0093)
22. Baier Leach J, Bivens KA, Patrick CW Jr, Schmidt CE (2003) Photocrosslinked hyaluronic acid hydrogels: natural, biodegradable tissue engineering scaffolds. *Biotechnol Bioeng* 82(5):578–589. doi:[10.1002/bit.10605](https://doi.org/10.1002/bit.10605)
23. Van Den Bulcke AI, Bogdanov B, De Rooze N, Schacht EH, Cornelissen M, Berghmans H (2000) Structural and rheological properties of methacrylamide modified gelatin hydrogels. *Biomacromolecules* 1(1):31–38. doi:[10.1021/bm990017d](https://doi.org/10.1021/bm990017d)
24. Ibusuki S, Halbesma GJ, Randolph MA, Redmond RW, Kochevar IE, Gill TJ (2007) Photochemically cross-linked collagen gels as three-dimensional scaffolds for tissue engineering. *Tissue Eng* 13(8):1995–2001. doi:[10.1089/ten.2006.0153](https://doi.org/10.1089/ten.2006.0153)
25. Dong CM, Wu XY, Caves J, Rele SS, Thomas BS, Chaikof EL (2005) Photomediated crosslinking of C6-cinnamate derivatized type-I collagen. *Biomaterials* 26(18):4041–4049. doi:[10.1016/j.biomaterials.2004.10.017](https://doi.org/10.1016/j.biomaterials.2004.10.017)
26. Poshusta AK, Anseth KS (2001) Photopolymerized biomaterials for application in the temporomandibular joint. *Cells Tissues Organs* 169(3):272–278
27. Brinkman WT, Nagapudi K, Thomas BS, Chaikof EL (2003) Photo-cross-linking of type-I collagen gels in the presence of smooth muscle cells: mechanical properties, cell viability, and function. *Biomacromolecules* 4(4):890–895. doi:[10.1021/Bm0257412](https://doi.org/10.1021/Bm0257412)
28. Sheu MT, Huang JC, Yeh GC, Ho HO (2001) Characterization of collagen gel solutions and collagen matrices for cell culture. *Biomaterials* 22(13):1713–1719
29. Damink LHH, Dijkstra PJ, van Luyn MJA, van Wachem PB, Nieuwenhuis P, Feijen J (1996) In vitro degradation of dermal sheep collagen cross-linked using a water-soluble carbodiimide. *Biomaterials* 17(7):679–684
30. Tenni R, Sonaggere M, Viola M, Bartolini B, Tira ME, Rossi A, Orsini E, Ruggeri A, Ottani V (2006) Self-aggregation of fibrillar collagens I and II involves lysine side chains. *Micron* 37(7):640–647. doi:[10.1016/j.micron.2006.01.011](https://doi.org/10.1016/j.micron.2006.01.011)
31. Lin DC, Dimitriadis EK, Horkay F (2007) Robust strategies for automated AFM force curve analysis: I. Non-adhesive indentation of soft, inhomogeneous materials. *J Biomech Eng-T Asme* 129(3):430–440. doi:[10.1115/1.2720924](https://doi.org/10.1115/1.2720924)
32. Walton RS, Brand DD, Czernuszka JT (2010) Influence of telopeptides, fibrils and crosslinking on physicochemical properties of Type-I collagen films. *J Mater Sci-Mater M* 21(2):451–461. doi:[10.1007/s10856-009-3910-2](https://doi.org/10.1007/s10856-009-3910-2)
33. Weadock KS, Miller EJ, Keuffel EL, Dunn MG (1996) Effect of physical crosslinking methods on collagen-fiber durability in proteolytic solutions. *J Biomed Mater Res* 32(2):221–226
34. Park SN, Park JC, Kim HO, Song MJ, Suh H (2002) Characterization of porous collagen/hyaluronic acid scaffold modified by 1-ethyl-3-(3-dimethylaminopropyl)carbodiimide cross-linking. *Biomaterials* 23(4):1205–1212
35. Williams CG, Malik AN, Kim TK, Manson PN, Elisseeff JH (2005) Variable cytocompatibility of six cell lines with photo-initiators used for polymerizing hydrogels and cell encapsulation. *Biomaterials* 26(11):1211–1218. doi:[10.1016/j.biomaterials.2004.04.024](https://doi.org/10.1016/j.biomaterials.2004.04.024)
36. Burdick JA, Anseth KS (2002) Photoencapsulation of osteoblasts in injectable RGD-modified PEG hydrogels for bone tissue engineering. *Biomaterials* 23(22):4315–4323 (pii:S0142-9612(02)00176-X)
37. Sundararaghavan HG, Monteiro GA, Firestein BL, Shreiber DI (2009) Neurite growth in 3D collagen gels with gradients of mechanical properties. *Biotechnol Bioeng* 102(2):632–643. doi:[10.1002/bit.22074](https://doi.org/10.1002/bit.22074)
38. Rault I, Frei V, Herbage D, AbdulMalak N, Huc A (1996) Evaluation of different chemical methods for cross-linking collagen gel, films and sponges. *J Mater Sci-Mater M* 7(4):215–221
39. Sundararaghavan HG, Monteiro GA, Lapin NA, Chabal YJ, Miksan JR, Shreiber DI (2008) Genipin-induced changes in collagen gels: Correlation of mechanical properties to fluorescence. *J Biomed Mater Res Part A* 87A(2):308–320. doi:[10.1002/jbm.a.31715](https://doi.org/10.1002/jbm.a.31715)
40. Elkin BS, Azeloglu EU, Costa KD, Morrison B (2007) Mechanical heterogeneity of the rat hippocampus measured by atomic force microscope indentation. *J Neurotraum* 24(5):812–822. doi:[10.1089/neu.2006.0169](https://doi.org/10.1089/neu.2006.0169)
41. Engler AJ, Sen S, Sweeney HL, Discher DE (2006) Matrix elasticity directs stem cell lineage specification. *Cell* 126(4):677–689. doi:[10.1016/j.cell.2006.06.044](https://doi.org/10.1016/j.cell.2006.06.044)
42. Lanza C, Morando S, Voci A, Canesi L, Principato MC, Serpero LD, Mancardi G, Uccelli A, Vergani L (2009) Neuroprotective mesenchymal stem cells are endowed with a potent antioxidant effect in vivo. *J Neurochem* 110(5):1674–1684. doi:[10.1111/j.1471-4159.2009.06268.x](https://doi.org/10.1111/j.1471-4159.2009.06268.x)